# Disturbance removal in passive radar via Sliding Extensive Cancellation Algorithm (ECA-S)

C. Palmarini, T. Martelli, F. Colone, P. Lombardo

DIET Dept., University of Rome "La Sapienza"
Via Eudossiana, 18 – 00184 Rome, Italy
e-mail: {palmarini, martelli, colone, lombardo}@diet.uniroma1.it

***Abstract*—In this paper an advanced version of the Extensive Cancellation Algorithm (ECA) is proposed for robust disturbance cancellation and target detection in passive radar. Firstly some specific limitations of previous ECA versions are identified when dealing with a highly time-varying disturbance scenario in the presence of slowly moving targets. Specifically, the need to rapidly adapt the filter coefficients is shown to yield undesired effects on low Doppler target echoes, along with the expected partial cancellation. Therefore a sliding version of the ECA is presented which operates on partially overlapped signals batches. The proposed modification to the original ECA is shown to appropriately counteract the limitations above by taking advantage of a smooth estimate of the filter coefficients. The benefits of the proposed approach are demonstrated against experimental data sets accounting for quite different passive radar applications.**

## I. INTRODUCTION

In recent years Passive Coherent Location (PCL) has received a great interest for the potential role it could play in both civilian and military applications [1]-[3]. In fact the parasitic exploitation of an existing illuminator inherently implies a low environmental impact and a covert operation. In this regard PCL systems can be regarded as "invisible" systems catching extremely weak signals (target echoes) that are usually "invisible" to the ordinary users of the employed transmitter. This is made possible by the use of receivers with wide dynamic range and by the application of appropriate signal processing techniques to tackle the invisibility of such weak target echoes against typical undesired signal contributions, above all the direct signal breakthrough and multipath. In this paper the term 'disturbance' is used throughout to indicate such undesired signals.

Indeed the disturbance cancellation represents one of the key stages within a conventional PCL processing scheme. To this purpose, the signal collected at the reference channel is usually exploited to remove undesired contributions, received together with the moving target echo, on the surveillance channel. Different approaches have been proposed to cope with this problem yielding solutions with different complexity and effectiveness [4]-[7].

Among these approaches, a largely used cancellation technique is the Extensive Cancellation Algorithm (ECA) and its Batches version (ECA-B) [7]-[14]. The ECA basically operates by subtracting, from the surveillance signal, delayed replicas of the reference signal properly weighted according to adaptively estimated coefficients. In its original version, the ECA requires the filter weights to be estimated by averaging over the whole coherent processing interval (CPI).

In contrast, the ECA-B approach estimates and applies the filter weights over smaller portions (batches) of the integration time. Reducing the temporal dimension of the single batch within certain limits does yield significant adaptivity loss when operating in a stationary environment. However, it was demonstrated in [7] to make the system more robust to the time-varying characteristics of the environment; this has been shown to be an appreciable advantage in many applications, especially when operating against non-stationary disturbance scenarios.

Nevertheless, the ECA-B might show some limitations when employed against highly time-varying disturbance scenarios in the presence of slowly moving targets. In fact the need for a rapid update of filter coefficients contrasts with the necessity to preserve the slowly moving target echo. In other words, using short batches widens the cancellation filter notch in the Doppler dimension yielding to a partial cancellation of the target return. Along with this obvious effect, we show that the batches operation yields undesired effects on the target echo at the output of the cancellation stage; such effects are then responsible for the emergence of unwanted structures in the range-Doppler map obtained at the output of the 2D cross-correlation between the reference and the surveillance signal.

Aiming at counteracting these limitations, we introduce a modified version of the ECA-B that operates over partially overlapped portions of the received signals. This ECA-Sliding (ECA-S) approach allows to separately set the update rate of the filter coefficients and the batch duration exploited for the adaptive estimation of the coefficients themselves. Therefore a better cancellation capability can be achieved by performing a rapid enough update of the filter weights; however the latter are obtained from longer and partially overlapped signal fragments in order to guarantee an accurate and smoothed estimation of the required coefficients.

The advantages yield by the proposed ECA-S approach are verified in this paper with reference to two live data sets accounting for very different PCL applications. Specifically a WiFi-based PCL is considered for target detection at short range aiming at local area surveillance. Moreover an FM-based PCL is employed for typical air traffic control (ATC) applications.

The paper is organized as follows. The limitations of the ECA and the ECA-B are investigated in Section II for short range and long range surveillance applications. The ECA-S approach is presented in Section III and its performance is analyzed in Section IV compared to previous approaches. Finally our conclusions are drawn in Section V.

## II. LIMITATIONS OF PREVIOUS ECA VERSIONS

As well known the ECA operates by subtracting from the surveillance signal $s_s(t)$ proper scaled and delayed replicas of the reference signal $s_r(t)$ [7]. Specifically, by sampling the received signals at $f_s$ and assuming that the multipath echoes are backscattered from the first *K* range bins, the output of the ECA is evaluated as:

$$s_{ECA}[n] = s_s[n] - \sum_{k=0}^{K-1} \alpha_k s_r[n-k] \quad n = 0, \dots, N-1 \tag{1}$$

where *N* is the number of samples within the CPI $T_{int}$. The filter coefficients $\boldsymbol{\alpha} = [\alpha_0 \ \alpha_1 \ \cdots \ \alpha_{K-1}]^T$ are evaluated by resorting to a Least Square (LS) approach that minimizes the power of the signal at the output of the filter:

$$\boldsymbol{\alpha} = (\mathbf{S}_r^{\mathrm{H}}\mathbf{S}_r)^{-1}\mathbf{S}_r^{\mathrm{H}}\mathbf{s}_s \tag{2}$$

where $\mathbf{s}_s$ is a $N \times 1$ vector containing *N* samples of the surveillance signal and $\mathbf{S}_r$ is a $N \times K$ matrix whose columns are the delayed versions of the reference signal. As is apparent, in its original version, the ECA requires the filter weights to be estimated over the whole CPI.

In contrast, the ECA-B output at the *l*-th batch is written as

$$s_{ECA-B}[n] = s_s[n] - \sum_{k=0}^{K-1} \alpha_k^{(l)} s_r[n-k]$$
$$n = lN_B, \dots, (l+1)N_B - 1; \ l = 0, \dots, \left\lfloor \frac{N}{N_B} \right\rfloor - 1 \tag{3}$$

where $N_B$ is the dimension of each batch and $\boldsymbol{\alpha}^{(l)} = \left[\alpha_0^{(l)} \ \alpha_1^{(l)} \ \cdots \ \alpha_{K-1}^{(l)}\right]^T$ is the filter coefficients estimate obtained at the *l*-th batch, namely by exploiting the *l*-th signal fragment of duration $T_B = N_B/f_s$. Basically we have

$$\boldsymbol{\alpha}^{(l)} = (\mathbf{S}_r^{(l)\mathrm{H}}\mathbf{S}_r^{(l)})^{-1}\mathbf{S}_r^{(l)\mathrm{H}}\mathbf{s}_s^{(l)} \tag{4}$$

where $\mathbf{s}_s^{(l)} = \left[s_s[lN_B], s_s[lN_B+1], \cdots, s_s[(l+1)N_B-1]\right]^T$ is a $(N_B \times 1)$ vector and $\mathbf{S}_r^{(l)}$ is a $N_B \times K$ matrix collecting the delayed copies of the corresponding reference signal fragment.

The ECA-B has been demonstrated to yield effective disturbance cancellation and target detection in a number of applications [7] ,[11]-[12]. Usually the batch duration $T_B$ has to be carefully selected as it affects the capability of the system to adapt to the time-varying characteristics of the environment. However, to avoid undesired effects, the need for a rapid update of filter coefficients has to be traded with the accuracy of the adaptive estimation and with the necessity of preserving the target echo. This point is shown in the following sub-sections with reference to quite different PCL applications.

### A. WiFi-based PCL for short range surveillance

In local area monitoring applications, WiFi transmissions might be successfully exploited [11]-[12]. Aiming at the detection of designated vehicles or human beings within public/private buildings and surrounding areas, it is quite typical to deal with targets observed at low Doppler frequency, namely slow-moving targets or targets moving mainly along the cross-range direction. Therefore it is of interest to study the effect of the ECA-B on the detection of such targets.

To this purpose we show the results obtained using the experimental setup described in [12]. In particular, a wireless access point (AP) was employed, set up to emit the beacon signal at 3 ms, and a quasi monostatic configuration was adopted for the surveillance and the transmitting antennas. Tests have been performed in a parking area using a vehicular target moving in the cross-range direction with approximate speed 4.5 m/s and distance of minimum approach $R_0$=20 m. In such geometry, the target describes a parabolic trajectory on the bistatic range-Doppler plane and, for a long time, it will be observed at Doppler frequencies within or close to the cancellation filter notch.

The acquired data have been processed via the processing scheme presented in [11]. Figs. 1 e 2 show the range-Doppler maps obtained after disturbance cancellation and sidelobes control with a CPI $T_{int}$ = 0.2 s for two different positions of the target along his trajectory. All the reported maps have been normalized to the thermal noise power level so that the value at each map location represents the estimated signal to noise ratio (SNR). Notice that the dynamic range has been lower limited to better highlight the main structures arising in the map. The adopted cancellation filter operates over a range extension of 250 m with different values of the batch duration $T_B$.

Specifically, Fig. 1 accounts for a favorable situation since the target Doppler frequency is reasonably high so that it is not affected by the cancellation stage. In fact, in this case, the ECA-B operates with $T_B$ = 100 ms that yields a notch Doppler extension equal to approximately $1/T_B$ which is significantly smaller than the target Doppler value. This batch duration has been experimentally verified to allow remarkable cancellation performance against the time-varying characteristics of the disturbance in this specific scenario. As a consequence, after the cancellation stage, the target appear as a strong peak at 53 m and -41 Hz. In addition, a further peak is also visible at 161 m and -33 Hz caused by the double-bounce reflection of the target echo over the metallic fence delimiting the parking area.

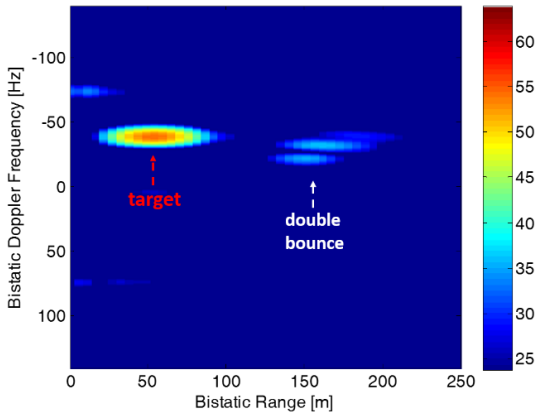


Fig. 1. Range-Doppler map after ECA-B with $T_B$ = 100 ms in the case of a high Doppler target.

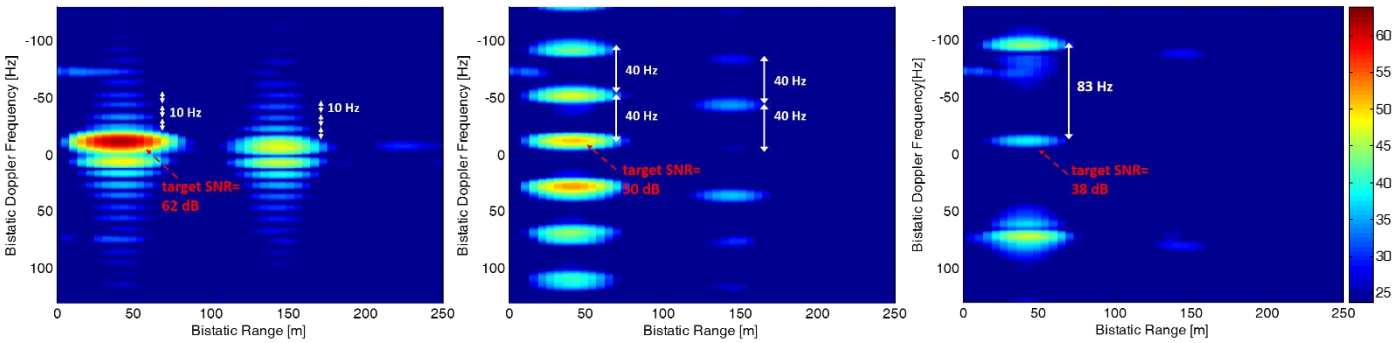


(a) (b) (c)

Fig. 2. Range-Doppler map after ECA-B for three different batch durations in the case of a low Doppler target: (a) $T_B$ = 100 ms; (b) $T_B$ = 25 ms; (c) $T_B$ = 12 ms.

In contrast, Fig. 2 shows the case of a target echo included in the filter cancellation notch so that it is expected to be strongly affected by the cancellation stage. In particular, Fig. 2(a-c) have been obtained by using batch durations equal to $T_B = 100$ ms, $T_B = 25$ ms, and $T_B = 12$ ms, respectively. As is apparent, in all cases, the target peak is surrounded by undesired structures in the Doppler dimension that might be responsible of useful dynamic range reduction or masking effects over weak targets, thus limiting the detection capability. These Doppler ambiguities are mainly due to the ECA-B approach that exploits consecutive batches of the received signals where the filter coefficients are separately estimated and applied. It can be shown that this yields discontinuities in the target echo at the output of this stage appearing at regular intervals of $T_B$ thus setting the Doppler spacing between unwanted peaks ($1/T_B$). Notice that in Fig. 2, as the batch duration decreases, the Doppler ambiguities spread accordingly. In addition, the cancellation notch is widened and the target SNR is progressively reduced.

Further decreasing $T_B$ would allow the undesired structures to be moved out of the Doppler range of interest. However this would also yield a more severe slowly-moving target removal and additional adaptivity loss since the disturbance characteristics would be estimated on few signal samples.

### *B. FM-based PCL for ATC applications*

In this section we investigate the effects of the ECA-B approach with reference to a long range surveillance application using the FM radio signal as waveform of opportunity. In this application, disturbance removal via ECA-B often provides excellent results making the system robust to slowly varying conditions of the observed scenarios.

Based on our experimental results [13]-[14], in this case quite long batch durations can be used which yield narrow cancellation notches compared to the typical high Doppler values of the aerial targets; as a consequence the adverse effects seen in the previous section occur with low probability, and, when this is the case, they appear for a very limited time thus not compromising the overall results.

However in severe scenarios (i.e. those characterized by rapidly varying disturbance characteristics, possibly induced by co- and inter-channel interference, severe multipath, transmitter dependent effects, etc.) it may be necessary to use batches of extremely small dimension to effectively remove the disturbance. Unluckily, this results in a considerable widening of the cancellation filter notch thus including even fast moving targets. As a result, the undesired effects shown in the previous section might arise limiting the surveillance capability of the PCL system.

To show this issue, we exploit the data set collected on June 7th 2012, in a site near the Fiumicino Airport. Receiver architecture and acquisition geometry are described in detail in [14]. Enough to know that two antennas were used: one antenna was employed to collect the reference signal and was steered toward the transmitter located on Monte Cavo, about 35 km South-East of the receiver site; the other antenna was pointed toward the opposite direction to gather the surveillance signal. Several sequential data acquisitions were performed for different FM radio channels; each acquisition is about 1.1 sec of duration, with a temporal spacing of about 2.3 sec between two consecutive acquisitions. A total time duration of about 4 minutes is considered in the following (100 data files). Live ATC (Air Traffic Control) registrations have been also collected for comparison.

All the available data files have been first processed according to a basic PCL processing scheme that includes: (i) disturbance (direct signal and multipath) cancellation using different ECA versions with $K$=140 taps (i.e. 210 km @ $f_s$ =200 kHz); (ii) evaluation of the two-dimensional cross-correlation function (2D-CCF) between the surveillance and the reference signal over a coherent processing interval (CPI) of 1 s; (iii) target detection via a cell-average constant false alarm rate (CA-CFAR) threshold with a nominal probability of false alarm $P_{fa}$=$10^{-4}$; (iv) track initiation using a conventional nearest neighbor association scheme with a '2 out of 2' strategy.

Using the conventional ECA for the disturbance removal, the results are those reported as red dots in Fig. 3, while black dots represent ATC registrations. Due to the high non-stationarity of the environment, resorting to the ECA-B approach allows better continuity in target detection. As an example, the results obtained with $T_B = 0.2$ s are reported in Fig. 4. Further decreasing the batch dimension (see Fig. 5 for $T_B = 0.025$ s) yields a further improvement of the detection capability since more complete plot sequences are detected and additional target tracks are correctly identified.

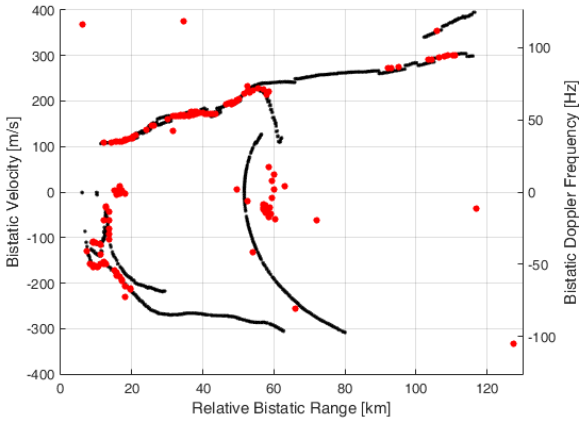


Fig. 3. Detected tracks after disturbance removal via ECA.

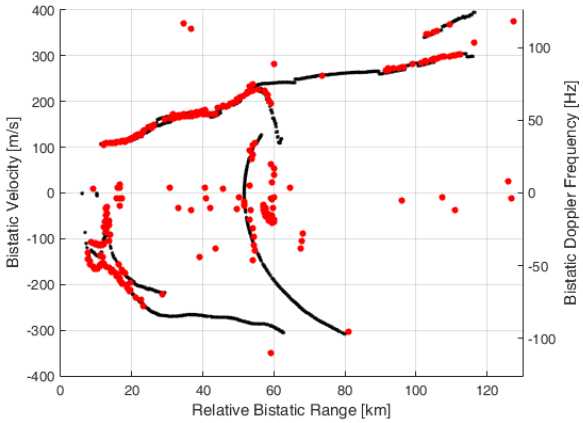


Fig. 4. Detected tracks after disturbance removal via ECA-B with $T_B = 0.2$ s.

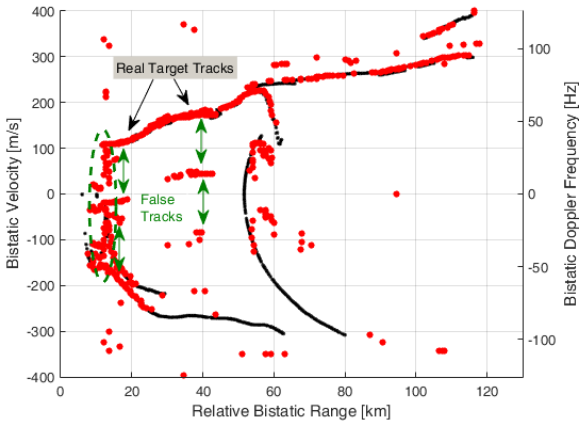


Fig. 5. Detected tracks after disturbance removal via ECA-B with $T_B = 0.025$ s.

However observe that the increased width of the cancellation filter notch might cause detection losses for targets crossing the zero Doppler. In addition, it is worth noticing that operating with $T_B = 0.025$ s yields a number of false tracks due to Doppler ambiguities at $1/T_B$ Hz distance from the corresponding true target track; this applies to the false targets appearing at near range around the zero Doppler.

## III. ECA-SLIDING

Based on the previous analysis, when the ECA-B approach is applied, special attention should be devoted to the selection of the batch duration as it affects both

- the capability to effectively remove the disturbance contributions possibly showing a non-stationary behavior and
- the possibility to nicely preserve the target echo.

Specifically the two requirements above might set opposite constraints on the selection of $T_B$. Long $T_B$ should be selected to reduce the minimum detectable velocity and to limit the adaptivity loss. In contrast, short $T_B$ should be preferred to be effective against disturbance with rapidly varying characteristics and to move the Doppler ambiguities out of the observed Doppler extent.

To overcome this limitation, we propose a sliding version of the ECA (ECA-S) which operates over partially overlapped signal fragments (see Fig. 6). This allows to decouple the selection of the batch duration exploited for the filter estimation and the update rate of the filter coefficients so that the requirements above could be jointly matched.

Basically a new parameter is introduced, $T_S$, that represents the signal fragment processed using a given filter; apparently, $T_S$ also coincides with the temporal separation between consecutive updates of the filter coefficients. Obviously, with the ECA-B approach we have $T_S = T_B$.

Thus ECA-S output at the *l*-th fragment is written as

$$s_{ECA-S}[n] = s_s[n] - \sum_{k=0}^{K-1} \alpha_k^{(l)} s_r[n-k]$$
$$n = lN_S, \dots, (l+1)N_S - 1;\ l = 0, \dots, \left\lfloor \frac{N}{N_S} \right\rfloor - 1 \qquad (5)$$

where $N_S$ is the dimension of each fragment (i.e. $N_S = T_S f_s$) and $\boldsymbol{\alpha}^{(l)} = \left[\alpha_0^{(l)}\ \alpha_1^{(l)}\ \cdots\ \alpha_{K-1}^{(l)}\right]^T$ are the current filter coefficients. These might be obtained by exploiting a longer signal fragment of duration $T_B = N_B/f_s$, symmetrically taken around the current signal fragment to be processed (see Fig. 6). Basically $\boldsymbol{\alpha}^{(l)}$ are evaluated as in (4) where the surveillance vector is given by

$$\mathbf{s}_s^{(l)} = \left[s_s\left[\left(l+\tfrac{1}{2}\right)N_S - \tfrac{N_B}{2}\right], s_s\left[\left(l+\tfrac{1}{2}\right)N_S - \tfrac{N_B}{2} + 1\right], \cdots,\right.$$
$$\left. s_s\left[\left(l+\tfrac{1}{2}\right)N_S + \tfrac{N_B}{2} - 1\right]\right]^T \quad (N_B \times 1) \qquad (6)$$

and $\mathbf{S}_r^{(l)}$ is a $N_B \times K$ matrix collecting the delayed copies of the corresponding reference signal batch.

Operating with this approach, the Doppler ambiguities associated to low Doppler targets are expected to appear with Doppler separation equal to $1/T_S$. Therefore, a reasonable strategy to design the parameters of the proposed cancellation filter is to select $T_B$ in order to allow remarkable cancellation performance against the time-varying characteristics of the disturbance for the specific operative scenario; this should be partly traded with the minimum detectable velocity to be guaranteed. In addition, $T_S$ can be selected as to move out of the Doppler range of interest [- $f_{Dmax}, f_{Dmax}$ ] the undesired

structures arising from the batch processing of the received signals, i.e. $T_S < \left(f_{Dmax} + \frac{1}{2T_B}\right)^{-1}$.

For example, with reference to two case studies considered in this paper, the following design criteria can be adopted:

- in the WiFi based PCL case, a batch duration $T_B = 100\,ms$ has been shown to be a good compromise for effective disturbance removal and reasonable target echo preservation. Moreover, as the maximum Doppler frequency observed is $f_{Dmax} = 130$ Hz, we might set $T_S < 7.4\,ms$.
- For the FM-based PCL, $T_B = 25\,ms$ has been experimentally verified to be a reasonable choice for the batch duration. In contrast, assuming a maximum velocity $v_{max} = 400\,m/s$ ($f_{Dmax} = 126$ Hz with the exploited FM radio channel at 94.5 MHz), we might set $T_S < 6.8\,ms$.

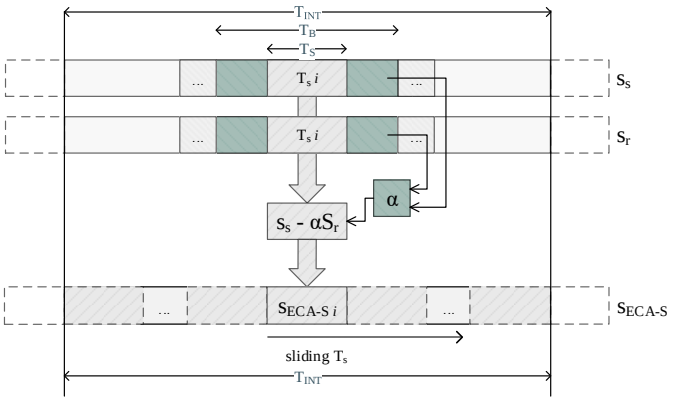


Fig. 6. Block diagram of ECA-S.

## IV. Experimental Results

The effectiveness of the sliding version of the ECA is shown in this section with reference to the case studies considered in Section II.

Figs. 7 and 8 report the results obtained after ECA-S, using the parameters $T_B$ and $T_S$ designed in the previous section, for the WiFi-based PCL and the FM-based PCL scenarios, respectively.

Specifically Fig. 7 shows the range-Doppler map obtained with the ECA-S for the same data set considered in Fig. 2. The adopted parameters are $T_B$ = 100 ms and $T_S$ = 3 ms; for a practical application, we set the filter update rate to be equal to the beacon emission rate of the exploited access point, i.e. the filter coefficients are updated beacon by beacon. Notice that the batch duration $T_B$ coincides with that used in Fig. 2(a). We observe that, with the adopted parameters, the new version of the ECA allows to move the Doppler ambiguities out of the Doppler extent of interest so that a single peak appear for the vehicular target (aside from the double-bounce contribution). However, exploiting a batch duration $T_B$ = 100 ms for the adaptive filter coefficients estimation yields an effective removal of the disturbance and allows to better preserve the slowly moving target echo. In fact the target SNR is slightly improved with respect to the ECA-B operating with $T_B$ = 100 ms.

Similarly, Fig. 8 reports the results of the detection and track initiation stages against the data set considered in Figs. 3-5 for a FM-base PCL system employed for ATC. In this case the ECA-S operates with $T_B = 25$ ms to guarantee an effective disturbance cancellation in the observed non-stationary environment. In contrast, using $T_S = 6.25$ ms allows to remove Doppler ambiguities appearing in the area of interest. As is apparent, comparable detection performance is obtained with respect to the application of the ECA-B approach operating with $T_B = 25$ ms; however, the possibility to separately set the updating rate allows to avoid the many false tracks appearing in Fig. 5.

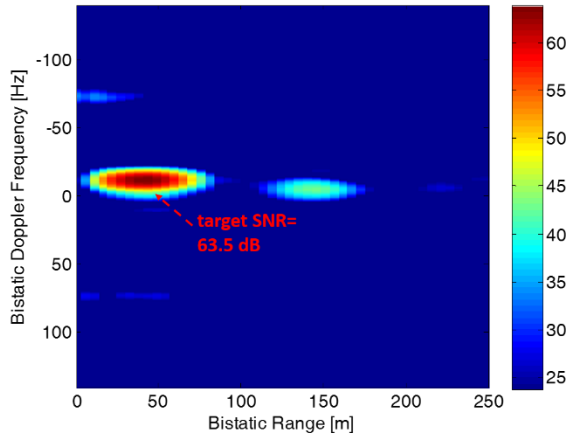


Fig. 7. Range-Doppler map after ECA-S for $T_B$ = 100 ms and $T_S$ = 3 ms.

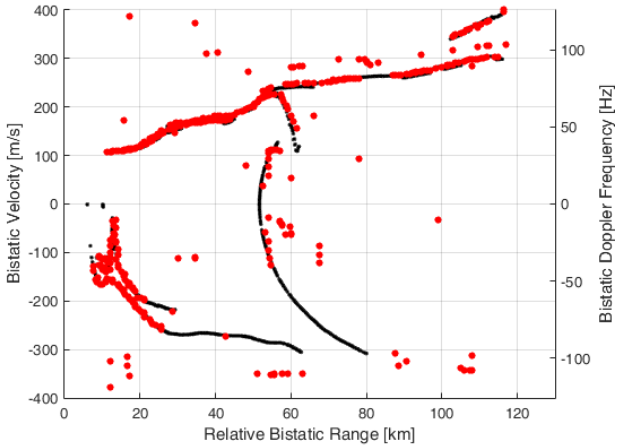


Fig. 8. Detected tracks after disturbance removal via ECA-S with $T_B = 0.025$ s and $T_S = 6.25$ ms.

Obviously the above advantages are paid in terms of computational burden since the filter weight computation is repeated a greater number of times within the CPI.

## V. CONCLUSIONS

In this paper, a modified version of the ECA-Batches has been presented to cope with some limitations observed when dealing with slowly-moving targets or targets moving mainly along the cross-range direction in passive radar. This ECA-Sliding approach operates on partially overlapped portions of the received signals so that it takes advantage of a smooth estimate of the filter coefficients.

The effectiveness of the proposed approach has been verified with reference to two live data sets accounting for very different PCL applications. In particular, a WiFi-based PCL for short range surveillance and a FM-based PCL for ATC application have been considered. The experimental results show that the ECA-S approach allows a better trade-off between disturbance cancellation and the capability to preserve low-Doppler target echoes thus improving the detection performance of the resulting PCL system.

## ACKNOWLEDGEMENT

Part of this work has been carried out under the support of the Project FP7-PEOPLE-2011-IAPP: SOS - "Sensors system for detection and tracking Of dangerous materials in order to increase the airport Security in the indoor landside area" funded by the European Union.

The authors gratefully acknowledge the collaboration of Dr. A. Macera and Dr. C. Bongioanni in setting up the experimental prototype and the acquisition campaigns.

## REFERENCES

[1] Special Issue on Passive Radar (Part I&II) – IEEE Aerospace and Electronic Systems Magazine, 2012, 27, (10-11), Guest Editors, A. Farina, H. Kuschel.

[2] Special Issue on Passive Radar Systems – IEE Proceedings on Radar, Sonar and Navigation, June 2005, 152, (3), Guest Editor P. Howland.

[3] Special issue on bistatic and MIMO radars and their applications in surveillance and remote sensing – IET Radar, Sonar & Navigation, 2014, 8, (2), Guest Editors A. Farina, M. Lesturgie.

[4] P.E. Howland, D. Maksimiuk, and G. Reitsma, "FM radio based bistatic radar," *IEE Proc. on Radar, Sonar and Navigation*, vol. 152, no. 3, June 2005.

[5] D. Poullin, "Passive detection using digital broadcasters (DAB, DVB) with COFDM modulation," *IEE Proc. on Radar, Sonar and Navigation*, vol. 152, no. 3, June 2005.

[6] K. Kulpa and Z. Czekala, "Masking effect and its removal in PCL radar," *IEE Proc. on Radar, Sonar and Navigation*, vol. 152, no. 3, June 2005.

[7] F. Colone, D. W. O'Hagan, P. Lombardo, and C. J. Baker, "A multistage processing algorithm for disturbance removal and target detection in Passive Bistatic Radar", IEEE Transactions on Aerospace and Electronic Systems, 2009, 45, (2), pp. 698-722.

[8] Z. Zhao, X. Wan, Q. Shao, Z. Gong, and F. Cheng, "Multipath clutter rejection for digital radio mondiale-based HF passive bistatic radar with OFDM waveform," *IET Radar, Sonar & Navigation*, vol. 6, no. 9, Dec. 2012.

[9] M.R. Inggs and C.A. Tong, "Commensal radar using separated reference and surveillance channel configuration", *Electronics Letters*, vol. 48, no. 18, 2012.

[10] L. Xiao-Yong, W. Jun, and W. Jue, "Robust direction of arrival estimate method in FM-based passive bistatic radar with a four-element Adcock antenna array," I*ET Radar, Sonar and Navigation*, vol. 9, no. 4, 2015

[11] F. Colone, P. Falcone, C. Bongioanni, and P. Lombardo, "WiFi-Based Passive Bistatic Radar: Data Processing Schemes and Experimental Results", IEEE Trans. on Aerospace and Electronic Systems, vol. 48, no. 2, April 2012, pp. 1061-1079.

[12] D. Pastina, F. Colone, T. Martelli, and P. Falcone, "Parasitic Exploitation of Wi-Fi Signals for Indoor Radar Surveillance," *Vehicular Technology, IEEE Transactions on* , vol.64, no.4, pp.1401,1415, April 2015.

[13] F. Colone, C. Bongioanni, and P. Lombardo, "Multi-Frequency Integration in FM Radio Based Passive Bistatic Radar. Part I: Target Detection", IEEE Aerospace and Electronic Systems Magazine, 2013, 28, (4), pp. 28-39.

[14] F. Colone, C. Bongioanni, and P. Lombardo, "Multi-Frequency Integration in FM Radio Based Passive Bistatic Radar. Part II: Direction of Arrival Estimation", IEEE Aerospace and Electronic Systems Magazine, 2013, 28, (4), pp. 40-47.